

Relaxation of A Thermally Bathed Harmonic Oscillator: A Study Based on the Group-theoretical Formalism

Yan Gu¹ and Jiao Wang^{2,3}

*¹Department of Modern Physics, University of Science
and Technology of China, Hefei 230026, Anhui, China*

*²Department of Physics and Fujian Provincial Key
Laboratory of Low Dimensional Condensed Matter Physics,
Xiamen University, Xiamen 361005, Fujian, China*

*³Lanzhou Center for Theoretical Physics,
Lanzhou University, Lanzhou 730000, Gansu, China*

(Dated: December 24, 2024)

arXiv:2412.16981v1 [quant-ph] 22 Dec 2024

Abstract

Quantum dynamics of a damped harmonic oscillator has been extensively studied since the sixties of the last century. Here, with a distinct tool termed the “group-theoretical characteristic function” (GCF), we investigate analytically how a harmonic oscillator immersed in a thermal environment would relax to its equilibrium state. We assume that the oscillator is at a pure state initially and its evolution is governed by a well-known quantum-optical master equation. By taking advantage of the GCF, the master equation can be transformed into a first-order linear partial differential equation that allows us to write down its solution explicitly. Based on the solution, it is found that, in clear contrast with the monotonic relaxation process of its classical counterpart, the quantum oscillator may demonstrate some intriguing nonmonotonic relaxation characteristics. In particular, when the initial state is a Gaussian state (i.e., a squeezed coherent state), it is found that there is a critical value of the environmental temperature, below which the entropy will first increase to reach its maximum value, then turn down and converge to its equilibrium value from above. For the temperature higher than the critical value, the entropy will converge to its equilibrium value from below monotonically. However, when the initial state is a Fock state, it is found that there is a new phase additional to the previous case, where the time curve of entropy features two extreme points. Namely, the entropy will increase to reach its maximum first, then turn down to reach its minimum, from where it begins to increase and converges to the equilibrium value eventually. Other related issues are discussed as well.

Keywords: Harmonic Oscillator; Quantum-optical Master Equation; Group-theoretical Characteristic Function.

I. INTRODUCTION

The evolution of a quantum system interacting with its environment is of fundamental importance in the theory of open quantum systems [1, 2]. In this paper, we study the evolution of a quantum harmonic oscillator moving irreversibly in a thermostatic surrounding. The reduced density matrix ρ of the oscillator is assumed to follow the quantum-optical master equation

$$\frac{d\rho}{dt} = -i\omega[a^\dagger a, \rho] + \Gamma(N_\beta + 1)(2a\rho a^\dagger - \{a^\dagger a, \rho\}) + \Gamma N_\beta(2a^\dagger \rho a - \{aa^\dagger, \rho\}), \quad (1)$$

where Γ is the damping constant, $\beta = \frac{1}{k_B T}$ with k_B and T being the Boltzmann constant and the environmental temperature, respectively, $N_\beta = (e^{\hbar\beta\omega} - 1)^{-1}$ is the expectation number of thermal quanta, and

$$a = \frac{1}{\sqrt{2\hbar M\omega}}(M\omega q + ip), \quad a^\dagger = \frac{1}{\sqrt{2\hbar M\omega}}(M\omega q - ip). \quad (2)$$

Retrospectively, in the early 1970s, this master equation had been derived by Louisell [3] for discussing a damped mode of the radiation field in a cavity and considered by Haake [4] as an example of the generalized master equation constructed by Nakajima and Zwanzig. Since then a large number of works have been devoted to this equation. Nowadays, it plays a central role not only for interpreting various quantum-optical experiments [5, 6], but also for studying environment-induced decoherence of open quantum systems [1]. On the other hand, it is also important to note that this equation provides only an approximate description of the motion of a physical oscillator, as having been remarked in literatures (see, e.g., p.17 of Ref. [7]). Thus one should be careful with its applicability in dealing with physical problems.

While it is generally not possible to solve Eq. (1) directly to find the solution $\rho(t)$ in the operator form, there are various methods to transform $\rho(t)$ into a c-number function (or distribution), in terms of which Eq. (1) can be transformed into a c-number equation, instead. One way is to take the Glauber-Sudarshan P representation [8, 9] resulted from representing the density operator as an ensemble of coherent states. An alternative approach is to use the Wigner distribution [10] or a phase-space quasi-probability distribution [11] that resembles more closely the classical probability distribution. After replacing the density operator $\rho(t)$ with these quasi-probability distributions, the operator master equation (1)

can be converted to a c-number Fokker-Planck equation [5–7, 12]. One skill to solve the resultant Fokker-Planck equation is to consider its Fourier transform (i.e., in terms of the characteristic function) [13], as Wang and Uhlenbeck did in developing the corresponding theory for a classical harmonic oscillator [14]. In fact, the differential equation in terms of the quantum characteristic function is a first-order linear partial differential equation. Its solution can be obtained with standard solving methods [5, 7, 12].

After solving Eq. (1), it is interesting to examine the relaxation process of the system starting from a pure quantum state towards the equilibrium state, a mixed state. This issue has been studied extensively as well (see Refs. [18–22] and references therein). For example, in Refs. [18, 19] the authors solved the relevant Fokker-Planck equation for the time dependent Wigner distribution and found that in the low temperature regime, the evolution of the quantum purity can exhibit non-monotonous behaviour for an initial Gaussian and or Fock state. In Refs. [20–22], the authors solved Eq. (1) via the quantum characteristic function of the density operator and analyzed in detail the relaxation properties revealed by the purity and other quantum metrics for various initial states. In particular, non-monotonous relaxation behaviours are found as well.

In a previous paper [15], we introduced a group-theoretical formalism of quantum mechanics. It requires that the Fourier transform of the density operator of a quantum system should be represented as a non-negative definite function on a group. This c-number function is termed as the “group-theoretical characteristic function (GCF)” of the density operator and the group it is defined on is termed as a “phase group” [15]. Under this Fourier-transform mapping, all observables (self-adjoint operators) of the system are mapped to Hermitian distributions with compact support and convolution multiplication on the group [16, 17], so that the non-commutativity of the observables is involved explicitly as a result of the non-commutativity of the group elements. In addition, the phase group for a system described with canonical variables is the well-known Heisenberg-Weyl group. Therefore, conceptually, this group-theoretical formalism and the characteristic function thus introduced should be more satisfactory from the perspective of physics. For applications, as we have the freedom to assign the group representation as well as the coordinates of the group manifold and in turn, the resultant form of the GCF, we have therefore the flexibility to choose the most convenient GCF form for solving a given problem.

In this paper, our motivations are twofold. The first is to review and to discuss the

group-theoretical formalism in studying the dynamical evolution of open quantum systems, in the hope that it may find more applications in future in view of its distinct advantages. The second is to use the GCF to solve Eq. (1) and bases on the solution, to identify the features peculiar to the quantum relaxation process of the damped harmonic oscillator, by comparison with the classical case. We shall show that, indeed, even for such a simple model, the quantum relaxation process may be much more diversifying compared with its classical counterpart. This part is scientifically interesting by itself, which is also an illustration of the effectiveness of the GCF approach in applications.

Mathematically, for the specific problem we are dealing with here, the GCF approach is equivalent to that in Refs. [20–22]. Here, in this paper, we will provide more and detailed discussions of the quantum relaxation process based on the analytical solutions of the master equation (1).

The organization of the remaining sections is as follows. In Sec. II, we will first introduce the GCF representation of a system described with canonical variables by making use of two different coordinate systems on the Heisenberg-Weyl group. They are related to the phase-space variables (\mathbf{q}, \mathbf{p}) and the complex variables $(\mathbf{a}, \mathbf{a}^\dagger)$, respectively. In Sec. III and Sec. IV, we present the relaxation phases of the damped harmonic oscillator with an initial Gaussian and an initial Fock state, respectively. The former is a squeezed coherent state and the latter is an energy eigenstate of the isolated harmonic oscillator. As a comparison with their classical counterparts, in Sec. V we will discuss the relaxation of the classical harmonic oscillator. Conclusions and discussions are given in Sec. VI. Finally, in Appendix, the analytical expression for describing the evolution of diagonal elements of the relevant density matrix in the Fock state basis is derived to illustrate the application of the GCF.

II. GCF REPRESENTATION AND QUANTUM-OPTICAL MASTER EQUATION

We start by considering a quantum system with a pair of canonical variables, (\mathbf{q}, \mathbf{p}) , and look upon the commutation relation $[\mathbf{q}, \mathbf{p}] = i\hbar$ as a Lie bracket of a three dimensional Heisenberg-Weyl Lie algebra [23]. This Lie algebra generates a nilpotent Lie group, denoted as $H(1)$ in the following. Let

$$g \rightarrow \mathbf{U}(g) = e^{i(x\mathbf{p} + y\mathbf{q} + z\hbar)}, \quad g \in H(1) \quad (3)$$

be an irreducible unitary representation of $H(1)$ on the state vector space \mathfrak{H} of the system, where $\{(x, y) \in \mathbb{R}^2, 0 \leq z < 2\pi/\hbar\}$ represents a canonical coordinate system on the group $H(1)$. Following Ref. [15], the GCF of the density matrix $\rho(t)$ of the quantum system at time t is defined as

$$\varphi(t, g) = \text{Tr}_{\mathfrak{H}}[\rho(t)\mathbf{U}(g)] \equiv e^{iz\hbar+v(x,y,t)} \quad (4)$$

with the inverse mapping

$$\rho(t) = \int_{H(1)} \varphi(t, g)\mathbf{U}^\dagger(g)dg, \quad (5)$$

where $dg = (\hbar/2\pi)^2 dx dy dz$ is the bi-invariant Haar measure on $H(1)$. If we use the complex variables $(\mathbf{a}, \mathbf{a}^\dagger)$ instead of (\mathbf{q}, \mathbf{p}) , the unitary representation of $H(1)$ in \mathfrak{H} has the form $\mathbf{U}(g) = e^{u\mathbf{a}^\dagger - \bar{u}\mathbf{a} + iz\hbar}$ with $u = u_1 + iu_2 = -\sqrt{\frac{\hbar M\omega}{2}}x + i\sqrt{\frac{\hbar}{2M\omega}}y$, which gives an alternative expression of the GCF

$$\varphi(t; g) = \text{Tr}_{\mathfrak{H}}[\rho(t)\mathbf{U}(g)] \equiv e^{iz\hbar+v(u,t)}. \quad (6)$$

Using the formulae $\mathbf{a}\mathbf{U}(g) = (-\frac{\partial}{\partial \bar{u}} + \frac{u}{2})\mathbf{U}(g)$ and $\mathbf{a}^\dagger\mathbf{U}(g) = (\frac{\partial}{\partial u} + \frac{\bar{u}}{2})\mathbf{U}(g)$, we can convert the quantum-optical master equation (1) into a c-number equation of $v(u, t)$ as

$$\frac{\partial v(u)}{\partial t} = -\{[(\Gamma u_1 + \omega u_2)\frac{\partial}{\partial u_1} + (\Gamma u_2 - \omega u_1)\frac{\partial}{\partial u_2}]v(u) + (1 + 2N_\beta)\Gamma|u|^2\}, \quad (7)$$

or, alternatively, of $v(x, y, t)$ as

$$\frac{\partial v(x, y)}{\partial t} = [(\frac{y}{M} - \Gamma x)\frac{\partial}{\partial x} - (M\omega^2 x + \Gamma y)\frac{\partial}{\partial y}]v(x, y) - \frac{\hbar}{2}(1 + 2N_\beta)\Gamma(M\omega x^2 + \frac{y^2}{M\omega}). \quad (8)$$

Note that Eqs. (7) and (8) are first-order linear partial differential equations that can be solved straightforwardly. Meanwhile, as shown in the following, the flexibility for generating different forms of the GCF by adopting different coordinates of the group manifold, and in turn, the different forms of the master equation [see Eqs. (7) and (8)], can be a remarkable advantage of the group-theoretical formalism in applications

III. RELAXATION OF AN INITIAL GAUSSIAN STATE

When the initial state of the system is a Gaussian state, $|\psi_G\rangle$, centered at (\bar{q}, \bar{p}) that

$$\langle q|\psi_G\rangle = (\frac{1}{2\pi\sigma^2})^{\frac{1}{4}} e^{-\frac{(q-\bar{q})^2}{4\sigma^2} + \frac{i}{\hbar}\bar{p}(q-\bar{q})}, \quad (9)$$

the GCF in terms of (x, y, z) [see Eq. (4)] is preferable for solving the corresponding master equation (8). For the initial density operator $\rho(0)$, the GCF reads $\varphi(0, g) = \langle \psi_G | \mathbf{U}(g) | \psi_G \rangle = e^{iz\hbar + v(x, y, 0)}$, where

$$v(x, y, 0) = i(x\bar{p} + y\bar{q}) - \left(\frac{\hbar^2 x^2}{8\sigma^2} + \frac{\sigma^2 y^2}{2} \right). \quad (10)$$

It is straightforward to verify that the solution of the master equation (8) with the initial condition (10) can be written down as

$$v(x, y, t) = A(t)x + B(t)y + a(t)x^2 + b(t)y^2 + c(t)xy, \quad (11)$$

where

$$\begin{cases} A(t) = ie^{-\Gamma t}(\bar{p} \cos \omega t - M\bar{q}\omega \sin \omega t), \\ B(t) = ie^{-\Gamma t}(\bar{q} \cos \omega t + \frac{\bar{p}}{M\omega} \sin \omega t), \\ a(t) = -\frac{\hbar M\omega}{4}(2N_\beta + 1)(1 - e^{-2\Gamma t}) - \frac{1}{2}e^{-2\Gamma t}\left(\frac{\hbar^2}{4\sigma^2} \cos^2 \omega t + M^2\sigma^2\omega^2 \sin^2 \omega t\right), \\ b(t) = -\frac{\hbar}{4M\omega}(2N_\beta + 1)(1 - e^{-2\Gamma t}) - \frac{1}{2}e^{-2\Gamma t}\left(\sigma^2 \cos^2 \omega t + \frac{\hbar^2}{4M^2\sigma^2\omega^2} \sin^2 \omega t\right), \\ c(t) = \frac{e^{-2\Gamma t}}{8M\sigma^2\omega}(4M^2\sigma^4\omega^2 - \hbar^2) \sin 2\omega t. \end{cases} \quad (12)$$

In the GCF representation, the purity of the system at time t has the form [15]

$$P(t) = \text{Tr}[\rho^2(t)] = \int_{H(1)} |\varphi(t, g)|^2 dg = \frac{\hbar}{2\pi} \int dx \int dy e^{2\text{Re}[v(x, y, t)]} \quad (13)$$

and in turn, for the initial Gaussian state (9), the linear entropy of the system is [24]

$$\begin{aligned} S(t) &= -\ln P(t) = \ln \frac{2}{\hbar} \sqrt{4a(t)b(t) - c(t)^2} \\ &= \frac{1}{2} \ln [e^{-4\Gamma t} + (1 - e^{-2\Gamma t})^2 (2N_\beta + 1)^2 + 2(1 - e^{-2\Gamma t})e^{-2\Gamma t} (2N_\beta + 1) \cosh 2r]. \end{aligned} \quad (14)$$

Here, the squeeze factor r is defined as $e^{-r} = \sigma/\sigma_c$, with $\sigma_c = \sqrt{\frac{\hbar}{2M\omega}}$. As we will discuss later in Sec. V, for a classical harmonic oscillator with an initially localized phase-space distribution, the time evolution of its entropy [see Eq. (49)] depends on neither the bath temperature nor its initial position in the phase space but the damping ratio $\Gamma/(2\omega)$. It is thus perplexing somehow to comprehend such differences between the quantum and the classical dynamical behaviour of the system in the context of non-equilibrium statistical mechanics.

To analyze Eq. (14) further, we first note that initially, $S(0) = 0$, and in the long time limit $t \rightarrow \infty$, $S(t) \rightarrow S_{eq} = \ln(2N_\beta + 1)$, regardless of the squeeze factor r of the initial state. It suggests that the system will relax to the equilibrium state, no matter what an

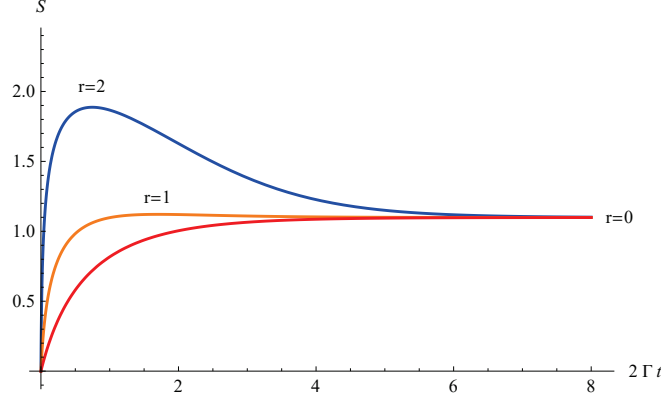


FIG. 1: The entropy as a function of time, $S(t)$, for an initial Gaussian state. The parameter N_β is fixed to be $N_\beta = 1$. From bottom to top, the red curve is for $r = 0$ and $N_c = 0$, the orange curve is for $r = 1$ and $N_c \approx 1.38$, and the blue curve is for $r = 2$ and $N_c \approx 13.15$. Note that $N_c = \sinh^2 r$.

initial Gaussian state it starts with. To characterize the proceeding relaxation process, the entropy production rate $R(t) = dS(t)/dt$ is a helpful tool. In particular, $R(0)$ can be used as a measure of the rate at which a pure state deteriorates into a mixture [25]. From Eq. (14), we have

$$R(0) = 2\Gamma[(2N_\beta + 1) \cosh 2r - 1], \quad (15)$$

suggesting that the minimum of the initial entropy production rate for a Gaussian state corresponds to the coherent state with $r = 0$. In other words, based on the quantum-optical master equation, the most stable Gaussian state for a thermally bathed harmonic oscillator is the coherent state. For this special case ($r = 0$), the entropy reads

$$S(t) = \ln[1 + 2N_\beta(1 - e^{-2\Gamma t})], \quad (16)$$

from which we can tell that the entropy of a coherent state will increase monotonically and saturate to its equilibrium value S_{eq} (see the red curve in Fig. 1).

For an initial state with $r \neq 0$, the behaviour of the entropy $S(t)$ becomes more complicated. To characterize $S(t)$, we consider the roots of $R(t) = 0$. It follows that for $N_\beta < N_c \equiv \sinh^2 r$, the only finite solution of $R(t) = 0$ is

$$t_m = \frac{1}{2\Gamma} \ln \left[\frac{2 + 4N_\beta + 4N_\beta^2 - 2(1 + 2N_\beta) \cosh 2r}{(1 + 2N_\beta)(1 + 2N_\beta - \cosh 2r)} \right], \quad (17)$$

when $S(t)$ adopts its maximum value

$$S_{max} = S(t_m) = \frac{1}{2} \ln \frac{(1 + 2N_\beta)^2 (\cosh^2 2r - 1)}{2[(1 + 2N_\beta)(\cosh 2r - 1) - 2N_\beta^2]}. \quad (18)$$

Note that S_{max} is greater than S_{eq} and increases monotonically as $|r|$. As a result, the time curve of the entropy features a ‘‘hump’’: The entropy will increase monotonically before t_m , then turn down to converge to S_{eq} from above monotonically (see, e.g., the blue curve in Fig. 1).

As t_m goes from $\frac{\ln 2}{2\Gamma}$ to ∞ as N_β increases from 0 to N_c , such a hump feature of $S(t)$ only shows up when $N_\beta < N_c$. For $N_\beta > N_c$, $S(t)$ will converge to S_{eq} monotonically from below. Therefore, N_c serves as a critical value that separates these two ‘‘phases’’ of the relaxation behavior that own qualitatively distinct characteristics. Note that $N_\beta = 1/(e^{\hbar\beta\omega} - 1)$ and $\beta = 1/(k_B T)$, we can determine from $N_\beta = N_c$ the critical environmental temperature T_c that separates these two phases physically: $T_c = \hbar\omega/[k_B \ln(1 + 1/\sinh^2 r)]$. For $N_\beta < N_c$, we have $T < T_c$

Now let us turn to the q -variance $(\Delta q)^2 = \text{Tr}[\rho q^2] - \text{Tr}[\rho q]^2$ to investigate how the quantum state spreads in the q space. Taking the GCF representation (4) and substituting Eq. (11), we have

$$(\Delta q)_t^2 = -\frac{\partial^2 v(x, y, t)}{\partial y^2} \Big|_{x=y=0} = -2b(t). \quad (19)$$

[See Eq. (12) for $b(t)$.] By introducing dimensionless variables $V = (\Delta q)^2/\sigma_c^2$ and $\gamma = \Gamma/\omega$, we can rewrite V as

$$V = V_1(N_\beta) + V_2(r, \gamma) \quad (20)$$

with

$$V_1 = (1 - e^{-2\Gamma t})(1 + 2N_\beta), \quad (21)$$

$$V_2 = e^{-2\Gamma t} \left[e^{-2r} \cos^2 \frac{\Gamma t}{\gamma} + e^{2r} \sin^2 \frac{\Gamma t}{\gamma} \right]. \quad (22)$$

Thus, we have $\langle (\Delta q)^2 \rangle_{t=0} = \sigma^2$ and $\langle (\Delta q)^2 \rangle_{t \rightarrow \infty} = (1 + 2N_\beta)\sigma_c^2$. Note that the squeeze factor r of the initial Gaussian state is contained in V_2 only, hence V_1 reflects a common spreading behavior followed by all Gaussian states and V_2 reflects the deviation from it for a given initial Gaussian state. Indeed, in the long time limit, $V_2 \rightarrow 0$ and the q -variance will be dominantly governed by V_1 exclusively.

For the particular case of $r = 0$ corresponding to an initial coherent state, the q -variance evolves as

$$\langle (\Delta q)^2 \rangle_t = [1 + 2N_\beta(1 - e^{-2\Gamma t})]\sigma_c^2, \quad (23)$$

which is non-decreasing, just as that for the classical harmonic oscillator thermally bathed.

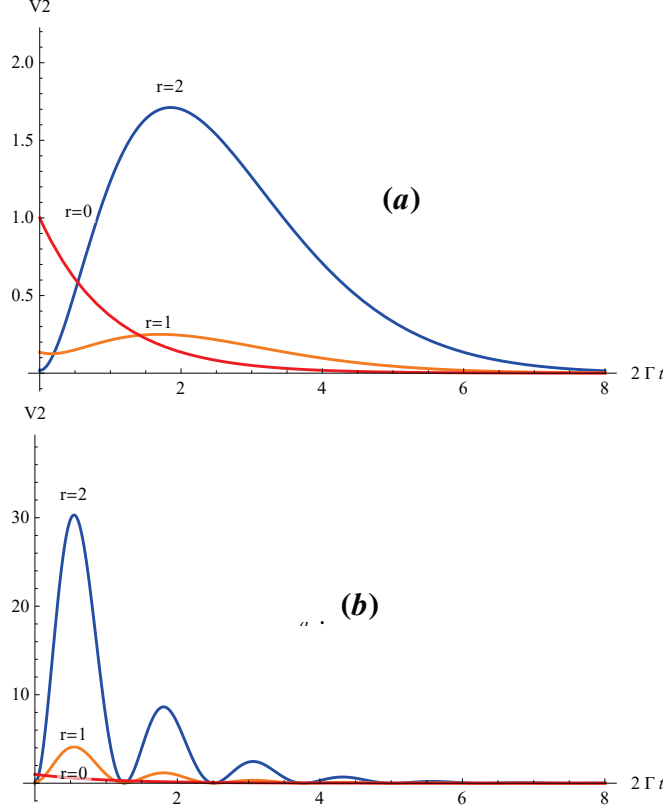


FIG. 2: Time function V_2 for an initial Gaussian state with $\gamma = 2$ (a) and $\gamma = 0.2$ (b). In both panels, the red line is for $r = 0$ and $\gamma_c = 0$, the orange line is for $r = 1$ and $\gamma_c \approx 3.626$, and the blue line if for $r = 2$ and $\gamma_c \approx 27.29$.

As the r.h.s of Eq. (23) does not depend on γ , the evolution of the q -variance is even simpler than its classical counterpart (see Sec. V).

For $r \neq 0$, the contribution of V_1 to the q -variance is the same as in the case of $r = 0$, but the oscillating term contained in V_2 will show up given that $\gamma < \gamma_c = \sinh 2|r|$. Similarly, zeros of the function

$$DV_2(t) = \frac{dV_2}{dt} = -\frac{2\Gamma}{\gamma} e^{-2(r+\Gamma t)} \left[\gamma \cos^2 \frac{\Gamma t}{\gamma} - (e^{4r} - 1) \cos \frac{\Gamma t}{\gamma} \sin \frac{\Gamma t}{\gamma} + e^{4r} \gamma \sin^2 \frac{\Gamma t}{\gamma} \right] \quad (24)$$

provide important information of V_2 . Suppose that $DV_2(t_m) = 0$ and let $\vartheta_m = \Gamma t_m / \gamma$, then equation $DV_2(t_m) = 0$ can be rewritten as

$$\gamma(\cot \vartheta_m + e^{4r} \tan \vartheta_m) = e^{4r} - 1, \quad (25)$$

which has real solutions ϑ_m if and only if $\gamma < \gamma_c = \sinh 2|r|$. Otherwise, V_2 is a monotonically decreasing function of time.

In Fig. 2 the time curves of $V_2(r, \gamma)$ for various values of r and γ are shown, where the characteristic behavior of V_2 and thus of the q -variance can be well appreciated. Note that for $\gamma < \gamma_c$, V_2 may have an increasing number of extremes as γ/γ_c decreases, implying that q -variance can be highly nonmonotonic in time.

IV. RELAXATION OF AN INITIAL FOCK STATE

When the initial state of the system is a Fock state, i.e., an energy eigenstate, $|n\rangle$, of the isolated harmonic oscillator system, it is preferable to take the complex coordinate system on $H(1)$ instead for solving the master equation. The corresponding GCF is

$$\varphi(g)|_{t=0} = \langle n|\mathbf{U}(g)|n\rangle = e^{izh + \frac{|u|^2}{2}} \langle n|e^{-\bar{u}\mathbf{a}} e^{u\mathbf{a}^\dagger}|n\rangle = e^{izh + v_n(u)}. \quad (26)$$

Note that, for the coherent state $|\alpha\rangle$, we have $\langle n|\alpha\rangle = \frac{\alpha^n}{\sqrt{n!}} e^{-\frac{|\alpha|^2}{2}}$, hence

$$\begin{aligned} \langle n|e^{-\bar{u}\mathbf{a}} e^{u\mathbf{a}^\dagger}|n\rangle &= \frac{1}{\pi n!} \int d^2\alpha |\alpha|^{2n} e^{-|\alpha|^2 + u\bar{\alpha} - \bar{u}\alpha} \\ &= \frac{e^{-|u|^2}}{\pi n!} \sum_{m=0}^n \binom{n}{m} \int d\alpha_1 \alpha_1^{2m} e^{-(\alpha_1 - iu_2)^2} \int d\alpha_2 \alpha_2^{2(n-m)} e^{-(\alpha_2 + iu_1)^2}. \end{aligned}$$

Using the formula $\int_{-\infty}^{\infty} dx x^n e^{-(x-y)^2} = \frac{\sqrt{\pi}}{(2i)^n} H_n(iy)$, we obtain that

$$v_n(u) \equiv v(u, 0) = \ln \left[\frac{(-1)^n}{n! 2^{2n}} e^{-\frac{1}{2}|u|^2} \sum_{m=0}^n \binom{n}{m} H_{2m}(u_2) H_{2(n-m)}(u_1) \right], \quad (27)$$

where $H_n(x)$ is the Hermite polynomial of degree n .

Now, we can write down the solution of the master equation (7) with the initial condition (27) as

$$v(u, t) = v_n(e^{-\Gamma t} u) + \frac{1}{2} (1 + 2N_\beta) (e^{-2\Gamma t} - 1) |u|^2 \quad (28)$$

and the entropy of the system as

$$S(t) = -\ln \left[\frac{1}{\pi} \int du_1 \int du_2 e^{2\mathbf{Re}[v(u,t)]} \right].$$

Making use of Eq. (28) and letting $a^2 = 1 + (1 + 2N_\beta)(e^{2\Gamma t} - 1)$, the entropy of the system (with $\rho(0) = |n\rangle\langle n|$) can be expressed further as

$$S_n(t) = -\ln \left[\frac{e^{2\Gamma t}}{(n! 2^{2n})^2 \pi} \sum_{m_1, m_2}^n \binom{n}{m_1} \binom{n}{m_2} IP(m_1, m_2) IP(n - m_1, n - m_2) \right], \quad (29)$$

where [26]

$$\begin{aligned}
IP(m_1, m_2) &= \int dx e^{-a^2 x} H_{2m_1}(x) H_{2m_2}(x) \quad (30) \\
&= 2^{2(m_1+m_2)} \Gamma(m_1 + m_2 + \frac{1}{2}) \frac{(1-a^2)^{m_1+m_2}}{a^{2(m_1+m_2)+1}} {}_2F_1(-2m_1, -2m_2, \frac{1}{2} - m_1 - m_2, \frac{a^2}{2(a^2-1)}) \quad (31)
\end{aligned}$$

From Eqs. (29) and (30), we have

$$S_n(0) = 0, \quad S_n(t)_{t \rightarrow \infty} = S_{eq} = \ln(1 + 2N_\beta), \quad (32)$$

the same as an initial Gaussian state as expected, and

$$\frac{dS_n}{dt} \Big|_{t=0} = 4\Gamma[(2n+1)N_\beta + n]. \quad (33)$$

We also note that the expression of $S_0(t)$ given by Eq. (29) is the same as that given by Eq. (16) for the coherent state, because the ground state $|0\rangle$ of an isolated harmonic oscillator is exactly the coherent state itself.

In general, the expression of $S_n(t)$ for $n > 0$ becomes more and more complicated as n grows. But in spite of this fact, qualitatively, $S_n(t)$ owns the same characteristics, regardless of n . For this reason, as an illustrating example, we will focus on $S_1(t)$ in the following. It reads

$$S_1(t) = \ln \left[\frac{[e^{-2\Gamma t} + (1 - e^{-2\Gamma t})(1 + 2N_\beta)]^3}{e^{-4\Gamma t} + (1 - e^{-2\Gamma t})^2(1 + 2N_\beta)^2} \right]. \quad (34)$$

To decode how the bath temperature T may affect $S_1(t)$, we check again the extreme points of $S_1(t)$ and see how they depend on N_β . Let $R_1(t) = dS_1(t)/dt$, we find the two roots of $R_1(t) = 0$ are

$$t_{\pm} = \frac{1}{2\Gamma} \ln \left[\frac{1 + 2N_\beta - 2N_\beta^2 - 4N_\beta^3 \pm \sqrt{1 + 6N_\beta + 10N_\beta^2 - 8N_\beta^4}}{(N_\beta - 1)(1 + 2N_\beta)^2} \right]. \quad (35)$$

So the necessary condition for $S_1(t)$ having extreme points is $N_\beta < N_c(1) \equiv 1 + d_1$, where $d_1 = \frac{1}{2}(\sqrt{3} - 1) \approx 0.366$. So $S_1(t)$ is non-decreasing only when $N_\beta > N_c(1)$. For $1 < N_\beta < N_c(1)$, there are two extreme points located at t_- and t_+ , respectively, and satisfying $S(t_-) > S_{eq} > S(t_+)$. As N_β decreases from $N_c(1)$ to 1, t_2 goes to infinity, hence $S_1(t)$ features a single maximum at t_- when $N_c(1) < 1$.

In short, compared with the case when the initial state is Gaussian, there is an additional phase of $S(t)$ for an initial Fock state. That is, when the environmental temperature satisfies $T_1 < T < T_c(1)$, $S(t)$ curve features two extreme points, where T_1 and $T_c(1)$ corresponds

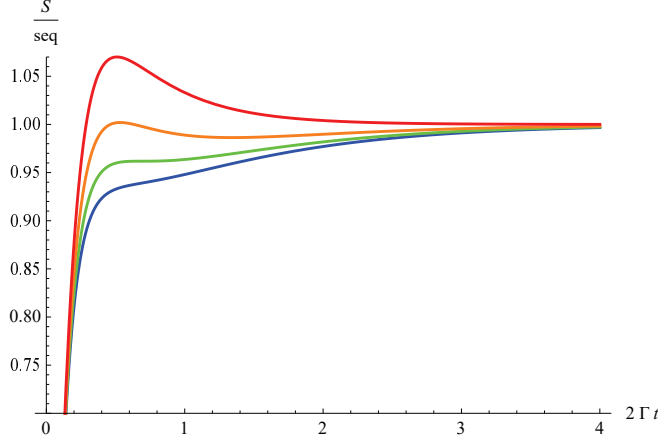


FIG. 3: Entropy $S_1(t)$ for the initial Fock state $|1\rangle$. From top to bottom, $N_\beta = 1.0$ (red), $N_\beta = 1.2$ (orange), $N_\beta = N_c(1) \approx 1.366$ (green), and $N_\beta = 1.5$ (blue). Note that the red and the green are the two critical curves, in between $S(t)$ features two extreme points (e.g., the orange curve).

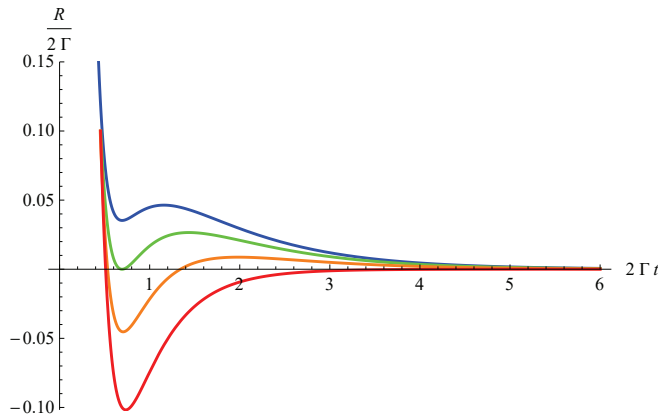


FIG. 4: The same as Fig. 3 but for $R(t)$ instead.

to $N_\beta = 1$ and $N_\beta = N_c(1)$, respectively. For $T < T_1$, $S(t)$ follows a hump, while for $T > T_c(1)$, $S(t)$ converges to S_{eq} from below monotonically. In Figs. 3 and 4, $S(t)$ and $R(t)$ are plotted, respectively, for four N_β values. The three-phase characteristics can be recognized straightforwardly.

Interestingly, it seems that such three-phase characteristics are shared by any Fock state $|n\rangle$, no matter how large n is. Now, the two critical temperatures correspond to $N_\beta = n$ and $N_\beta = N_c(n)$ instead, where $N_c(n) = n + d_n$ with d_n being a positive number increasing with n . Specifically, numerical computation suggests that $d_2 \approx 0.645$ and $d_3 \approx 0.924$, respectively. Again, for $N_\beta > N_c(n)$ and $N_\beta < n$, we have the monotonic converging phase

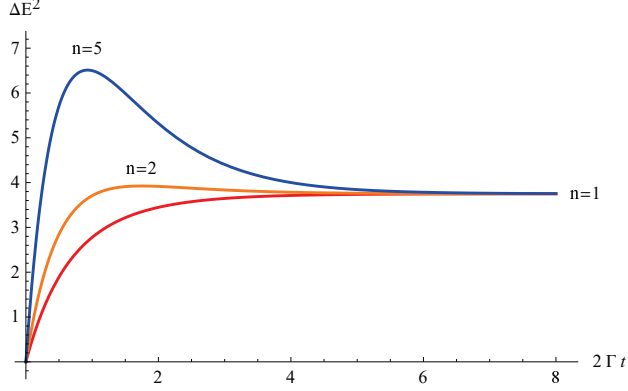


FIG. 5: Energy variance $\langle(\Delta E)^2\rangle$ as a function of time for $N_\beta = 1.5$. The three curves, from bottom to top, are for $n = 1$ (red), $n = 2$ (orange), and $n = 5$ (blue), respectively.

and the hump phase, respectively, while for $n < N_\beta < N_c(n)$, $S_n(t)$ is dominated by the two extreme points. When N_β decreases from $N_c(n)$ to n , the time t_+ corresponding to the right, minimum point tends to infinity.

It is also interesting to see how the energy spreads in the energy space. To this end, it is convenient to consider the energy variance. Note that in the GCF representation, we have

$$\text{Tr}_{\mathfrak{H}}[\rho a^\dagger a] = \langle a^\dagger a \rangle = \left[\frac{|u|^2}{4} - \frac{1}{4} \left(\frac{\partial^2}{\partial u_1^2} + \frac{\partial^2}{\partial u_2^2} \right) - \frac{i}{2} \left(u_1 \frac{\partial}{\partial u_2} - u_2 \frac{\partial}{\partial u_1} \right) - \frac{1}{2} \right] e^{v(u)} \Big|_{u=0}. \quad (36)$$

By introducing the dimensionless variable $E = a^\dagger a + \frac{1}{2}$ and making use of Eq. (28), we have straightforwardly that

$$\langle E \rangle = N_\beta + \frac{1}{2} + (n - N_\beta) e^{-2\Gamma t}, \quad (37)$$

$$\langle (\Delta E)^2 \rangle = (1 - e^{-2\Gamma t}) [N_\beta(1 + N_\beta) - e^{-2\Gamma t} (N_\beta^2 - 2nN_\beta - n)]. \quad (38)$$

Furthermore, since the root of $d\langle(\Delta E)^2\rangle/dt = 0$ is

$$t_m = \frac{1}{2\Gamma} \ln \left[1 + \frac{n(1 + 2N_\beta) + N_\beta}{(n - N_\beta)(1 + 2N_\beta)} \right], \quad (39)$$

we conclude that there are two phases of $\langle(\Delta E)^2\rangle$: For $N_\beta > n$, it has no extreme point and therefore it will monotonically increase from 0 and saturate to its equilibrium value $\langle(\Delta E)^2\rangle_{eq} = N_\beta(1 + N_\beta)$. Whereas for $N_\beta < n$, the time curve of the energy variance features a hump; it will first increase from 0 to its maximum

$$\langle(\Delta E)^2\rangle_{max} = \frac{(n(1 + 2N_\beta) + N_\beta)^2}{4(n(1 + 2N_\beta) - N_\beta^2)} \quad (40)$$

and then tends monotonically to $\langle(\Delta E)^2\rangle_{eq}$. The time curves of the energy variance for three different n values are plotted in Fig. 5 as an illustration.

V. RELAXATION OF THE CLASSICAL DAMPED HARMONIC OSCILLATOR

In order to better appreciate the peculiarity due to the quantum effects in the relaxation process of the quantum harmonic oscillator, here we investigate the relaxation process of its classical counterpart as a comparative study. We assume that for a classical damped harmonic oscillator, its relaxation towards the thermal equilibrium is a Gaussian random process and the evolution of its probability distribution $\rho(q, p, t)$ in phase space (q, p) at time t is governed by the Fokker-Planck equation (see Eq. (51) in Ref. [14])

$$\frac{d\rho}{dt} = \left\{ -\frac{p}{M} \frac{\partial}{\partial q} + \frac{\partial}{\partial p} [M\omega^2 q + \Gamma(p + k_B T M \frac{\partial}{\partial p})] \right\} \rho. \quad (41)$$

Parallel to our discussion in the quantum case, by taking advantage of the classical characteristic function of $\rho(q, p, t)$ defined as

$$\varphi(x, y, t) = \int dq \int dp e^{i(xp+qy)} \rho(q, p) \equiv e^{v(x, y, t)}, \quad (42)$$

the Fokker-Planck equation (41) can be transformed into a first-order inhomogeneous linear partial differential equation of $v(x, y, t)$,

$$\frac{\partial v(x, y, t)}{\partial t} = \left[\left(\frac{y}{M} - \Gamma x \right) \frac{\partial}{\partial x} - M\omega^2 x \frac{\partial}{\partial y} \right] v(x, y, t) - \Gamma k_B T M x^2. \quad (43)$$

For the initially localized probability distribution $\rho(q, p, 0) = \delta(q - \bar{q})\delta(p - \bar{p})$,

$$v(x, y, 0) = i(\bar{p}x + \bar{q}y), \quad (44)$$

the solution of Eq. (43) with the initial condition (44) can be written down as

$$v(x, y; t) = \tilde{A}(t)x + \tilde{B}(t)y + \tilde{a}(t)x^2 + \tilde{b}(t)y^2 + \tilde{c}(t)xy, \quad (45)$$

where

$$\begin{cases} \tilde{A}(t) = \frac{ie^{-\frac{\Gamma t}{2}}}{2\alpha^2} [2\bar{p}(\alpha^2 \cosh \frac{\alpha\Gamma t}{2} - \alpha \sinh \frac{\alpha\Gamma t}{2}) + M\Gamma\bar{q}(\alpha^2 - 1)\alpha \sinh \frac{\alpha\Gamma t}{2}], \\ \tilde{B}(t) = \frac{ie^{-\frac{\Gamma t}{2}}}{M\Gamma\alpha^2} [2\bar{p}\alpha \sinh \frac{\alpha\Gamma t}{2} + M\Gamma\bar{q}(\alpha^2 \cosh \frac{\alpha\Gamma t}{2} + \alpha \sinh \frac{\alpha\Gamma t}{2})], \\ \tilde{a}(t) = -\frac{Mk_B T e^{-\Gamma t}}{2\alpha^2} [\alpha^2(e^{\Gamma t} - 1) + 1 - \cosh \alpha\Gamma t + \alpha \sinh \alpha\Gamma t], \\ \tilde{b}(t) = -\frac{2e^{-\Gamma t} k_B T}{M\Gamma^2 \alpha^2 (1 - \alpha^2)} [\alpha^2(e^{\Gamma t} - 1) + 1 - \cosh \alpha\Gamma t - \alpha \sinh \alpha\Gamma t], \\ \tilde{c}(t) = -\frac{2e^{-\Gamma t} k_B T}{\Gamma\alpha^2} (\cosh \alpha\Gamma t - 1). \end{cases} \quad (46)$$

Note that in Eq. (46), we have used the dimensionless parameter $\alpha \equiv \sqrt{1 - \frac{4\omega^2}{\Gamma^2}}$ instead of the frequency ω for convenience. Thus, the oscillator is underdamped for α being imaginary or overdamped for α being real ($0 < \alpha \leq 1$).

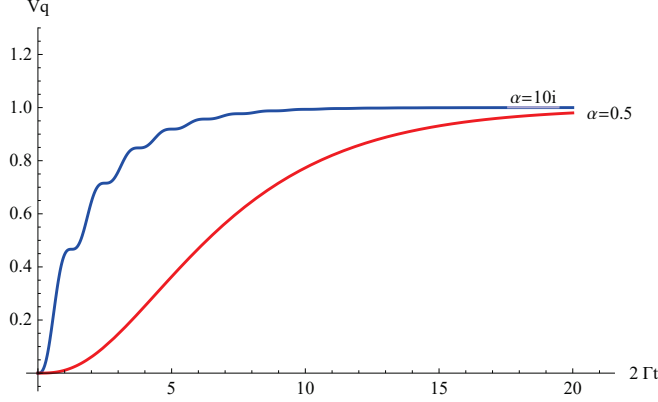


FIG. 6: Time dependence of the position variance of the classical damped harmonic oscillator with a localized initial condition. The bottom red curve is for an overdamped case with a real α (0.5) and the top blue curve is for an underdamped case with an imaginal α ($10i$), respectively.

In terms of the characteristic function, the position variance of the oscillator reads

$$\langle(\Delta q)^2\rangle_t = -2\tilde{b}(t) = \frac{4kT}{M\Gamma^2\alpha^2(1-\alpha^2)}[\alpha^2 + e^{-\Gamma t}(1-\alpha^2 - \cosh \alpha\Gamma t - \alpha \sinh \alpha\Gamma t)], \quad (47)$$

which is seemingly the same as Eq. (19) for the quantum case by simply replacing $b(t)$ with $\tilde{b}(t)$. It follows that $\langle(\Delta q)^2\rangle_0 = 0$ and $\langle(\Delta q)^2\rangle_{eq} = \frac{k_B T}{M\omega^2}$. Furthermore, as

$$\frac{d\langle(\Delta q)^2\rangle_t}{dt} = \frac{4kT e^{-\Gamma t}(\cosh \alpha\Gamma t - 1)}{\alpha^2 M\Gamma} \geq 0,$$

the classical q -variance is non-decreasing for the localized initial condition discussed here. In Fig. 6, $Vq \equiv \langle(\Delta q)^2\rangle_t / \langle(\Delta q)^2\rangle_{eq}$ is adopted for showing two examples for the overdamped case ($\alpha = 0.5$) and the underdamped case ($\alpha = 10i$), respectively.

In contrast with the monotonic behavior of q -variance, the evolution of energy variance can be much more complicated. In fact, the E -variance $\langle(\Delta E)^2\rangle = \langle E^2\rangle - \langle E\rangle^2$ can be worked out by making use of the following formulae:

$$\langle E\rangle_t = \mathfrak{L}[e^{v(x,y;t)}]|_{x=y=0}, \quad \langle E^2\rangle_t = \mathfrak{L}^2[e^{v(x,y;t)}]|_{x=y=0},$$

where $\mathfrak{L} = -[\frac{1}{2M}\frac{\partial^2}{\partial x^2} + \frac{M\omega^2}{2}\frac{\partial^2}{\partial y^2}]$ is a differential operator on the characteristic function.

Without loss of generality, let $\bar{q} = 0$ and $\bar{p} = \sqrt{2ME_0}$. For convenience, let us introduce the dimensionless parameter $\lambda \equiv E_0/(k_B T)$ and set $V(t) = \frac{\langle(\Delta E)^2\rangle_t}{(k_B T)^2}$. We find that there exists a critical value of λ , denoted as λ_c , which is a function of α , such that for $\lambda < \lambda_c$, $V(t)$ relaxes monotonically from 0 to 1, whereas for $\lambda > \lambda_c$, $V(t)$ evolves in an oscillatory way.

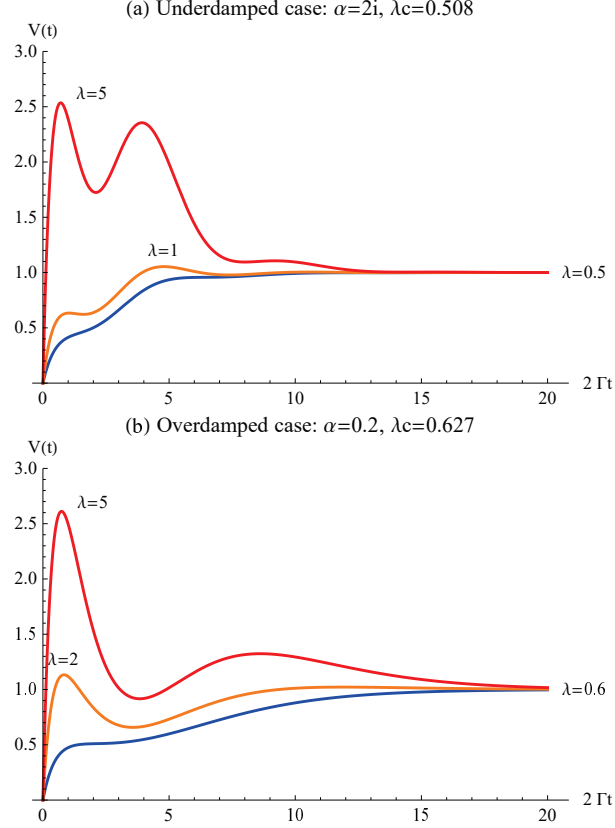


FIG. 7: Time dependence of the energy variance of the classical damped harmonic oscillator for the underdamped case with $\alpha = 2i$ and $\lambda_c \approx 0.508$ (a) and the overdamped case with $\alpha = 0.2$ and $\lambda_c \approx 0.627$ (b). In (a), from bottom to top, the three curves are for initial energy $E_0 = \lambda k_B T$ with $\lambda = 0.5$ (blue), $\lambda = 1$ (orange), and $\lambda = 5$ (red), respectively, while in (b), from bottom to top, the three curves are for $\lambda = 0.6$ (blue), $\lambda = 2$ (orange), and $\lambda = 5$ (red), respectively.

In Fig. 7, $V(t)$ for various initial energy values are shown for both the underdamped and the overdamped cases. It can be seen that, in both cases the E -variance could be highly nonmonotonic.

Finally, let us discuss the entropy of the classical damped harmonic oscillator. Considering Eqs. (42) and (45), the entropy can be expressed as

$$\begin{aligned}
 S(t) &= -\ln[h \int dq \int dp \rho^2(q, p)] \\
 &= \ln \frac{4\pi^2}{h} - \ln \int dx \int dy e^{2\text{Re}[v(x, y, t)]} \\
 &= \ln \frac{4\pi}{h} + \frac{1}{2} \ln[4\tilde{a}(t)\tilde{b}(t) - \tilde{c}^2(t)],
 \end{aligned} \tag{48}$$

where h is a constant independent of t . Inserting Eq. (46) into Eq. (48) and considering a

specific value of h for convenience, i.e., $h = 4\pi k_B T / \Gamma$, we have

$$S(t) = \frac{1}{2} \ln \left[\frac{4(2e^{-\Gamma t} + \alpha^2(1 - e^{-\Gamma t})^2 - 2e^{-\Gamma t} \cosh \alpha \Gamma t)}{\alpha^2(1 - \alpha^2)} \right]. \quad (49)$$

Note that $S(t)$ given by (49) does not depend on the bath temperature, but it has a pathological point at $t = 0$ that does not appear in the quantum case. To avoid this defect, we can turn to considering the coarse-grained probability distribution $\rho_c(q, p)$ instead, which may be written in the form of [27]

$$\rho_c(q, p) = \frac{1}{2\pi\sigma_q\sigma_p} \int dQ \int dP e^{-\left(\frac{Q^2}{2\sigma_q^2} + \frac{P^2}{2\sigma_p^2}\right)} \rho(q - Q, p - P).$$

Setting the characteristic function of $\rho_c(q, p, t)$ as $e^{v_c(x, y, t)}$, we have

$$v_c(x, y, t) = v(x, y, t) - \frac{1}{2}(\sigma_p^2 x^2 + \sigma_q^2 y^2), \quad (50)$$

the coarse-grained entropy of the system thus reads

$$S_c(t) = \frac{1}{2} \ln \left[4(\tilde{a}(t) - \frac{1}{2}\sigma_p^2)(\tilde{b}(t) - \frac{1}{2}\sigma_q^2) - \tilde{c}^2(t) \right]. \quad (51)$$

Considering that the general properties of the coarse-grained entropy should not be affected by the coarse-graining details, for our aim here it is convenient to adopt a certain specific value of the coarse-graining size. In particular, by setting $\sigma_q^2 = \frac{k_B T}{M\Gamma^2}$ and $\sigma_p^2 = Mk_B T$, we obtain that

$$S_c(t) = \frac{1}{2} \ln \left[\frac{2(5 - \alpha^2)}{1 - \alpha^2} + \frac{13 - \alpha^2}{\alpha^2} e^{-\Gamma t} + \frac{4}{1 - \alpha^2} e^{-2\Gamma t} + e^{-\Gamma t} \frac{(\alpha^2 - 13) \cosh \alpha \Gamma t - \alpha(3 + \alpha^2) \sinh \alpha \Gamma t}{\alpha^2(1 - \alpha^2)} \right], \quad (52)$$

from which it follows that

$$S_c(0) = 0; \quad S_c(t)|_{t \rightarrow \infty} = \frac{1}{2} \ln \frac{2(5 - \alpha^2)}{1 - \alpha^2}. \quad (53)$$

Moreover, by further analyzing $S(t)$ in detail, we find that the coarse-grained entropy $S_c(t)$ is actually a non-decreasing function and satisfies the requirement of the generalized H -theorem. As an illustration, in Fig. 8 the time derivative of $S_c(t)$, $R(t) \equiv dS_c(t)/dt$, is displayed for the cases when the oscillator is underdamped, critically damped, and overdamped, respectively. Note that in all the three cases, $R(t) > 0$ for a finite t and $R(t) \rightarrow 0$ as $t \rightarrow \infty$, suggesting that $S_c(t)$ relaxes to its equilibrium value monotonically from below.

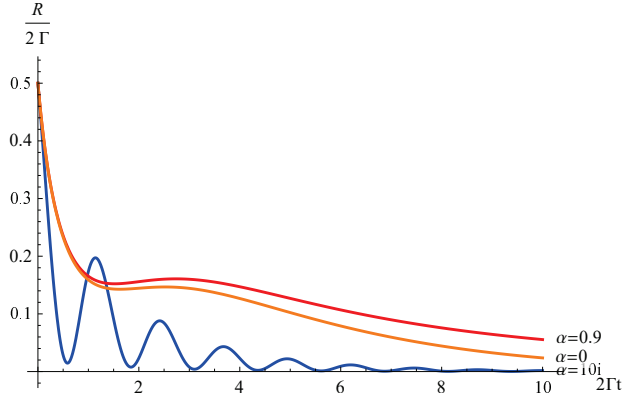


FIG. 8: Plot of the time derivative of the coarse-grained entropy $R(t) \equiv dS_c(t)/dt$ for the classical harmonic oscillator when it is underdamped with $\alpha = 10i$ (blue), critically damped with $\alpha = 0$ (orange), and overdamped with $\alpha = 0.9$ (red), respectively.

VI. SUMMARY AND DISCUSSIONS

We have demonstrated that, starting from a pure quantum state, the evolution of the harmonic oscillator governed by the quantum-optical master equation may have some unusual features in the course of thermalization.

The main findings by studying the entropy $S = -\ln \text{Tr}[\rho^2]$ are: *I.* For an initial Gaussian state, there exists a critical value of N_β , i.e., $N_c = \sinh^2 r$ (or equivalently a critical temperature of the thermal bath), such that if $N_\beta = (e^{\hbar\beta\omega} - 1)^{-1} > N_c$, the entropy will relax monotonically from 0 to its equilibrium value $S_{eq} = \ln(1 + 2N_\beta)$, whereas when $N_\beta < N_c$, the entropy will increase first to $S_{max}(r)$ (an infinitely increasing function of the squeeze factor r), then approaches asymptotically to its equilibrium value S_{eq} ; *II.* For an initial Fock state $|n\rangle$ with $n > 0$, there are two critical values of N_β instead, one is n and another is $N_c = n + d_n$, where d_n is a positive number. As a result, an additional new phase of $S(t)$ appears for $n < N_\beta < N_c$, where $S(t)$ is dominated by a pair of extreme points in between $S(t)$ decreases. *III.* In addition, the entropy of the quantum oscillator does not depend explicitly on its frequency ω , in contrast with the classical case where ω plays a role and distinctive features for underdamping and overdamping cases manifest. Moreover, the classical entropy is independent of the bath temperature.

We would like to remark that, assuming the entropy defined as $S = -\ln \text{Tr}[\rho^2]$ (proposed by Prigogine [24]) rather than the von Neumann entropy $S = -\text{Tr}[\rho \ln \rho]$, facilitates greatly

our analytical calculations. But note that, unlike the von Neumann entropy, the former may fail to reflect some aspects of entropy, such as concavity and subadditivity [28], and as a result it can not provide the information of the correlations between the subsystem and the reservoir [29]. However, as a function of state, the Prigogine entropy serves well as a measure of the purity or dispersity of a mixed state. For these two reasons, the Prigogine entropy is ideal for our aim here to probe the relaxation process from a pure state towards a mixed state.

Finally, we discuss two possible ways for determining the valid range of our theoretical predictions based on the quantum-optical master equation.

I. By comparison with the related experimental studies.

As entropy is not an observable, for a comparison with experimental study, it is advisable to extract information about the dynamical evolution from experimentally accessible quantities. In view of the recent progress in experimental studies on QND photon counting as well as the dynamical evolution of photon number distribution of a relaxing optical field (e.g., Refs. [30–32]), in Appendix we show that the evolution of the photon number distribution can be solved analytically by taking the GCF representation. Particularly, in Appendix the case when the initial state is a Gaussian state is discussed in detail, which might be useful for a comparison with the experimental results.

II. By comparison with the results predicted by more sophisticated master equations.

Extensive studies have been conducted in recent decades on refining the Lindblad master equation from various aspects in order to better capture the evolution of an open quantum system. For example, constructing the generalized master equation for describing the dynamics beyond the Markov approximation [33]; recovering positivity of the Redfield equation via the partial secular approximation [34]; correcting the Redfield equation by using the exact mean-force Gibbs state [35]. Further studies based on these generalized master equations should be helpful. If the found relaxation phases and the transition between them remain, then we will have more faith that they are true properties of the open quantum harmonic oscillator.

Appendix A: Evolution of diagonal elements of the density matrix in the Fock state basis

In order to facilitate the comparison between the theoretical predictions based on the master equation Eq. (5) and the experimental studies, here we discuss the evolution of the diagonal elements of the density operator in the Fock state basis. The GCF turns to be very helpful for this aim as well.

We denote the state of a quantum optical field by the density matrix $\rho(t)$ and set its GCF as $\varphi(g) = e^{iz\hbar+v(u,t)}$. According to Eq. (5), the diagonal elements of $\rho(t)$ in the Fock state basis can be written as

$$P(n, t) \equiv \langle n | \rho(t) | n \rangle = \frac{1}{\pi} \int d^2 u e^{v(u,t) + \overline{v_n(u)}}, \quad (\text{A1})$$

where $v_n(u)$ is given by Eq. (27). Since for the thermal state we have $v_{eq}(u) = -\frac{1}{2}(1 + 2N_\beta)|u|^2$, it is easy to verify that

$$P(n, t)|_{t \rightarrow \infty} = \frac{1}{\pi} \int d^2 u e^{v_{eq}(u) + \overline{v_n(u)}} = \frac{N_\beta^n}{(1 + N_\beta)^{n+1}}.$$

When the initial state is a Gaussian state (given by Eq. (9)) and the dynamical evolution of the system governed by Eq. (1), we may use the following transformation

$$\bar{q} = 2\sigma_c \alpha_1, \quad \bar{p} = \frac{\hbar \alpha_2}{\sigma_c}, \quad x = -\frac{2\sigma_c u_1}{\hbar}, \quad y = \frac{u_2}{\sigma_c}, \quad \sigma = \sigma_c e^{-r}, \quad (\text{A2})$$

to rewrite Eqs. (10) and (11) as

$$v(u, 0) = 2i(\alpha_1 u_2 - \alpha_2 u_1) - \frac{1}{2}(e^{2r} u_1^2 + e^{-2r} u_2^2), \quad (\text{A3})$$

$$v(u, t) = A_u(t)u_1 + B_u(t)u_2 + a_u(t)u_1^2 + b_u(t)u_2^2 + c_u(t)u_1u_2, \quad (\text{A4})$$

where

$$\begin{cases} A_u(t) = -2ie^{-\Gamma t}(\alpha_2 \cos \omega t - \alpha_1 \sin \omega t), \\ B_u(t) = 2ie^{-\Gamma t}(\alpha_1 \cos \omega t + \alpha_2 \sin \omega t), \\ a_u(t) = -\frac{1}{2}e^{-2\Gamma t}((e^{2\Gamma t} - 1)(2N_\beta + 1) + e^{2r} \cos^2 \omega t + e^{-2r} \sin^2 \omega t), \\ b_u(t) = -\frac{1}{2}e^{-2\Gamma t}((e^{2\Gamma t} - 1)(2N_\beta + 1) + e^{-2r} \cos^2 \omega t + e^{2r} \sin^2 \omega t), \\ c_u(t) = e^{-2\Gamma t} \sinh 2r \sin 2\omega t. \end{cases} \quad (\text{A5})$$

As $\langle n | [a^\dagger a, \rho] | n \rangle = 0$, according to Eq. (1), $P(n, t)$ does not depend explicitly on the parameter ω . To facilitate the calculation of $P(n, t)$, we can construct an ancillary density

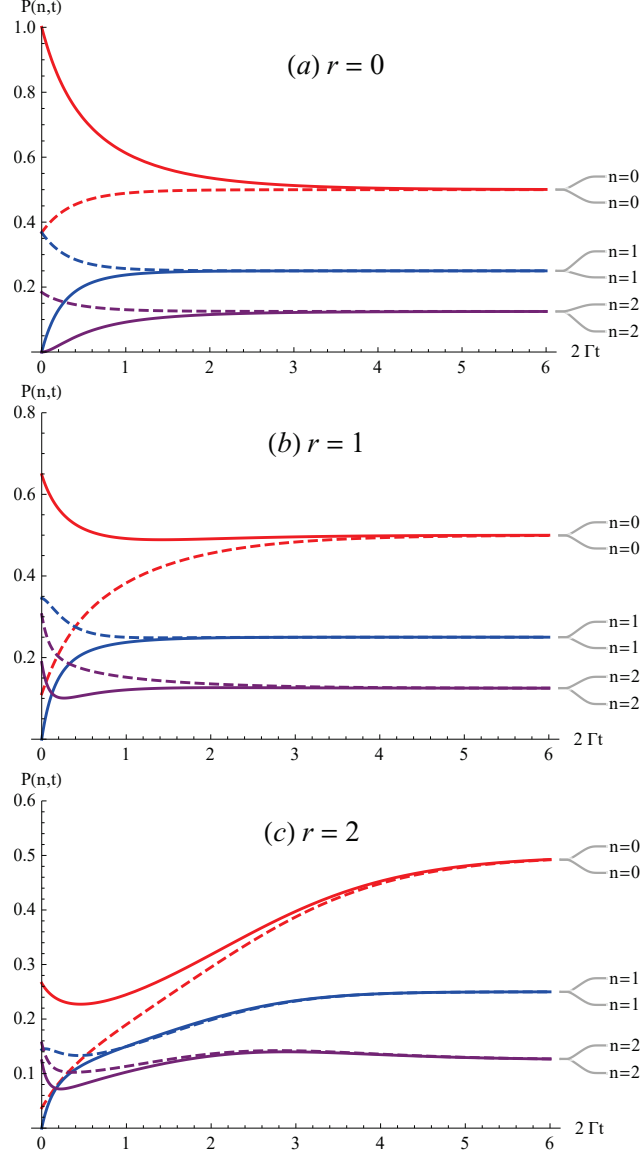


FIG. 9: Function $P(n,t)$ for an initial squeezed coherent state with $N_\beta = 1$ and $\alpha_2 = 0$. From top to bottom, the three panels are for $r = 0$ (a), $r = 1$ (b), and $r = 2$ (c), respectively. In all panels, the solid (dashed) lines are for $\alpha_1 = 0$ ($\alpha_1 = 1$). The n value for each curve is labeled at its right side.

matrix $\rho_1(\mathbf{t})$ satisfying the master equation

$$\frac{d\rho_1}{dt} = \Gamma(N_\beta + 1)(2a\rho_1 a^\dagger - \{a^\dagger a, \rho_1\}) + \Gamma N_\beta(2a^\dagger \rho_1 a - \{a a^\dagger, \rho_1\}), \quad (\text{A6})$$

so that $P_1(n,t) \equiv \langle n|\rho_1(t)|n\rangle = P(n,t)$ if initially we have $P_1(n,0) = P(n,0)$.

Let the GCF of $\rho_1(t)$ be $\varphi_1(g) = e^{izh+v_1(u,t)}$. If initially $v_1(u,0) = v(u,0)$, we have

$$v_1(u,t) = A_1(t)u_1 + B_1(t)u_2 + a_1(t)u_1^2 + b_1(t)u_2^2 + c_1(t)u_1u_2, \quad (\text{A7})$$

where

$$\begin{cases} A_1(t) = -2ie^{-\Gamma t}\alpha_2, \\ B_1(t) = 2ie^{-\Gamma t}\alpha_1, \\ a_1(t) = -\frac{1}{2}e^{-2\Gamma t}((e^{2\Gamma t} - 1)(2N_\beta + 1) + e^{2r}), \\ b_1(t) = -\frac{1}{2}e^{-2\Gamma t}((e^{2\Gamma t} - 1)(2N_\beta + 1) + e^{-2r}), \\ c_1(t) = 0. \end{cases} \quad (\text{A8})$$

Thus we can rewrite Eq. (A1) as

$$P(n, t) = \frac{1}{\pi} \int d^2u e^{v_1(u, t) + \overline{v_n(u)}} = \frac{(-1)^n}{\pi 2^{2n}} \sum_{m=0}^n \frac{1}{m!(n-m)!} \times \int du_1 H_{2(n-m)}(u_1) e^{A_1(t)u_1 + (a_1(t) - \frac{1}{2})u_1^2} \int du_2 H_{2m}(u_2) e^{B_1(t)u_2 + (b_1(t) - \frac{1}{2})u_2^2}. \quad (\text{A9})$$

Using the integral formula

$$\int_{-\infty}^{\infty} dx H_n(x) e^{-a^2 x^2 + bx} = \frac{\sqrt{\pi}(a^2 - 1)^{\frac{n}{2}} e^{\frac{b^2}{4a^2}}}{a^{n+1}} H_n\left(\frac{b}{2a\sqrt{a^2 - 1}}\right), \quad \text{for } a > 0, \quad (\text{A10})$$

we then have

$$P(n, t) = \frac{(-1)^n}{2^{2n}} e^{\frac{A_1(t)^2}{4d_1^2} + \frac{B_1(t)^2}{4d_2^2}} \sum_{m=0}^n \frac{1}{m!(n-m)!} \frac{(d_1^2 - 1)^{n-m} (d_2^2 - 1)^m}{d_1^{2(n-m)+1} d_2^{2m+1}} \times H_{2(n-m)}\left(\frac{A_1(t)}{2d_1\sqrt{d_1^2 - 1}}\right) H_{2m}\left(\frac{B_1(t)}{2d_2\sqrt{d_2^2 - 1}}\right), \quad (\text{A11})$$

where $d_1 = \sqrt{\frac{1}{2} - a_1(t)}$ and $d_2 = \sqrt{\frac{1}{2} - b_1(t)}$.

Equation (A11) gives analytically the evolution of the photon number distribution $P(n, t)$ based on the quantum-optical master equation (1), where its dependence on the initial state parameter α and the squeeze factor r [36] is indicated explicitly. In Fig. 9, several cases for various parameter values are plotted, where the overall characteristics of $P(n, t)$ can be recognized.

To show further the dependence of $P(n, t)$ on N_β , let us discuss a simple case: the relaxation process of $P(0, t)$ (i.e., $n = 0$) for a squeezed vacuum. According to Eq. (A11), for a squeezed vacuum we have

$$P(0, t) = \frac{1}{\sqrt{\frac{1}{2} - a_1(t)} \sqrt{\frac{1}{2} - b_1(t)}}. \quad (\text{A12})$$

The time dependence of $P(0, t)$ can be characterized by zeros of equation $R(t) = dP(0, t)/dt$. It is found that the only finite solution is

$$t_m = \frac{1}{2\Gamma} \ln\left[\frac{1 + 2N_\beta + 2N_\beta^2 - (1 + 2N_\beta) \cosh 2r}{2(1 + N_\beta)(N_\beta - \sinh^2 r)}\right]. \quad (\text{A13})$$

Therefore, when N_β increases from 0 to $N_c = \sinh^2 r$, t_m will increase from 0 to ∞ . Note that $R(0) \leq 0$, $P(0, t)$ bends downward if and only if $N_\beta < \sinh^2 r$, as shown in Fig. 9. It is interesting to note that, for this special case, the critical value of N_β is the same as that given in Sec. III for the relaxation of entropy. However, for the cases where $n \neq 0$ and/or $\alpha \neq 0$, the dependence of $P(n, t)$ on N_β becomes quite complicated.

-
- [1] H. P. Breuer and F. Petruccione, *The Theory of Open Quantum Systems* (Oxford University Press, Oxford, 2002).
 - [2] D. Weiss, *Quantum Dissipative Systems* (World Scientific, Singapore, 2000).
 - [3] W. H. Louisell, *Quantum Statistical Properties of Radiation* (John Wiley & Sons, New York, 1973).
 - [4] F. Haake, *Statistical Treatment of Open Systems by Generalized Master Equations*, Springer Tracts in Modern Physics, Vol.66 (Springer, Berlin, 1973).
 - [5] D. F. Walls and G. J. Milburn, *Quantum Optics* (Springer, 2008).
 - [6] O. Miguel, *Quantum Optics* (Springer, 2007).
 - [7] H. J. Carmichael, *Statistical Methods in Quantum Optics 1* (Springer, 2002).
 - [8] R. J. Glauber, Phys. Rev. **131**, 2776 (1963).
 - [9] E. C. G. Sudarshan, Phys. Rev. Lett. **10**, 277 (1963).
 - [10] E. Wigner, Phys. Rev. **40**, 749 (1932).
 - [11] G. S. Agarwal and E. Wolf, Phys. Rev. D **2**, 2187 (1970).
 - [12] H. Risken, *The Fokker Planck Equation*, Appendix A4 (Springer, 1989).
 - [13] R. von Mises, *Mathematical Theory of Probability and Statistics* (Academic, New York, 1964).
 - [14] M. C. Wang and G. E. Uhlenbeck, Rev. Mod. Phys. **17**, 323 (1945).
 - [15] Y. Gu, Phys. Rev. A **32**, 1310 (1985).
 - [16] Y. Gu, Science in China A **35**, 200 (1992).
 - [17] Y. Gu, *Quantum Statistical Mechanics, Quantum Probability and Quantum Characteristic Function*(in Chinese), Sci. China-Phys. Mech. Astron. **50**, 070002 (2020).
 - [18] V. V. Dodonov, S. S. Mizrahl, and A. L. de Souza Silva, J. Opt. B: Quantum and Semiclassical Optics **2**, 271 (2000).
 - [19] J. P. Valeriano and V. V. Dodonov, Phys. Lett. A **384**, 126370 (2020).

- [20] P. Marian and T. A. Marian, Phys. Rev. A **47**, 4474 (1993).
- [21] P. Marian and T. A. Marian, Phys. Rev. A **47**, 4487 (1993).
- [22] P. Marian, I. Ghiu, and T. A. Marian, Phys. Rev. A **88**, 012316 (2013).
- [23] K. B. Wolf, *The Heisenberg-Weyl Ring in Quantum Mechanics*, in *Group Theory and Its Applications* Vol. III, p.189, edited by E. M. Loeb (Academic Press, New York, 1975).
- [24] I. Prigogine, *Time, Irreversibility and Structure*, in *The Physicist's Conception of Nature* p.579, edited by J. Mehra (Reidel, Dordrecht 1973).
- [25] W. H. Zurek, S. Habib, and J. P. Paz, Phys. Rev. Lett. **70**, 1187 (1993).
- [26] L. S. Gradshteyn and L. M. Ryzhik, *Table of Integrals, Series and Products*, p.837 (formula 7.374-5), (Academic Press, New York, 1980).
- [27] Y. Gu, Phys. Lett. A **149**, 95 (1990).
- [28] A. Wenrl, Rev. Mod. Phys. **50**, 221 (1978).
- [29] M. Esposito, K. Lindenberg, and C. van den Breck, New J. Phys. **12**, 013013 (2010).
- [30] M. Brune, S. Haroche, V. Lefevre, J. M. Raimond and N. Zagury, Phys. Rev. Lett. **65**, 976 (1990).
- [31] C. Guerlin, J. Bernu, S. Deleglise, C. Sayrin, S. Gleyzes, S. Kuhr, M. Brune, J. M. Raimond, and S. Haroche, Nature **448**, 889 (2007).
- [32] M. Brune, J. Bernu, C. Guerlin, S. Deleglise, C. Sayrin, S. Gleyzes, S. Kuhr, I. Dotsenko, J. M. Raimond, and S. Haroche, Phys. Rev. Lett. **101**, 240402 (2008).
- [33] I. de Vega and D. Alonso, Rev. Mod. Phys. **89**, 015001 (2017).
- [34] D. Farina and V. Giovannetti, Phys. Rev. A **100**, 012107 (2019).
- [35] T. Becker, A. Schnell, and J. Thingna, Phys. Rev. Lett. **129**, 200403 (2022).
- [36] An explicit expression of the generating function $G(z, t)$ of the photon number distribution $P(n, t)$ for an initial Gaussian state has been given by Eq. (53) in Ref. [18].